Research report

EEG based zero-phase phase-locking value (PLV) and effects of spatial filtering during actual movement

Wenjuan Jian [a,*], Minyou Chen [a], Dennis J. McFarland [b]

[a] State Key Laboratory of Power Transmission Equipment & System Security and New Technology, School of Electrical Engineering, Chongqing University, Chongqing, China
[b] National Center for Adaptive Neurotechnologies, Wadsworth Center, New York State Department of Health, Albany, NY, USA

ABSTRACT

Phase-locking value (PLV) is a well-known feature in sensorimotor rhythm (SMR) based BCI. Zero-phase PLV has not been explored because it is generally regarded as the result of volume conduction. Because spatial filters are often used to enhance the amplitude (square root of band power (BP)) feature and attenuate volume conduction, they are frequently applied as pre-processing methods when computing PLV. However, the effects of spatial filtering on PLV are ambiguous. Therefore, this article aims to explore whether zero-phase PLV is meaningful and how this is influenced by spatial filtering. Based on archival EEG data of left and right hand movement tasks for 32 subjects, we compared BP and PLV feature using data with and without pre-processing by a large Laplacian. Results showed that using ear-referenced data, zero-phase PLV provided unique information independent of BP for task prediction which was not explained by volume conduction and was significantly decreased when a large Laplacian was applied. In other words, the large Laplacian eliminated the useful information in zero-phase PLV for task prediction suggesting that it contains effects of both amplitude and phase. Therefore, zero-phase PLV may have functional significance beyond volume conduction. The interpretation of spatial filtering may be complicated by effects of phase.

© 2017 Elsevier Inc. All rights reserved.

1. Introduction

Network models (Bullmore and Sporns, 2009; Stam and van Straaten, 2012) have gained popularity within neuroscience in recent years. This has led to interest in measures such as coherence (Carter et al., 1973) and phase-locking value (PLV) (Lachaux et al., 1999) as measures of EEG connectivity. However, there is concern about the possible role of volume conduction in EEG studies of functional connectivity. Volume conduction refers to the fact that the conductive properties of the brain, skull, and the soft tissue result in the spatial smearing of EEG signals. As a result, volume conduction can produce high values of coherence and PLV at zero-phase difference between spatially close electrode pairs. Therefore, investigators have proposed coupling measures such as the imaginary part of coherence (Nolte et al., 2004) and phase lag index (Stam et al., 2007), both of which eliminate information near zero phase differences so as to negate the effects of volume conduction. An alternative strategy to deal with volume conduction effects makes use of spatial filtering (e.g., (Nunez et al., 2015; Tenke and Kayser, 2015)).

Movement or imagery of movement results in a change in the ongoing EEG activity over central scalp locations that is not phase-locked to these events (Pfurtscheller and Lopes da Silva, 1999). These effects are frequency-band specific, occurring in the 9–13 Hz (mu) and 18–25 Hz (beta) range. Collectively they are called sensorimotor rhythms (SMRs) due to their reactivity to movement and movement-related phenomena. Typically, there is a suppression of oscillatory activity in areas overlying sensorimotor cortex associated with the active body part (desynchronization, or ERD) and occasionally an increase in surrounding areas or as a rebound phenomenon after movement (synchronization, or ERS). People can learn to control the sensorimotor rhythm ERD/ERS in these areas in order to control a cursor on a video screen or a virtual space (McFarland et al., 2010; Wolpaw et al., 1991; Wolpaw and McFarland, 2004).

Andrew and Pfurtscheller (1996) observed an increase in mu rhythm coherence between the hemispheres with movement,

which they suggested was due to volume conduction as it was largely eliminated by spatial filtering with a Laplacian derivation. Nunez et al. (2015, 2001, 1999, 1997) support the application of surface Laplacian for eliminating volume conduction in EEG connectivity analysis. Tenky and Kayser (2015) also recommend use of a surface Laplacian in the study of coherence. For error-related functional connectivity study, Cohen (2015a) demonstrated that the surface Laplacian is likely to be the best spatial transformation in reducing volume conduction. Wei et al. (2007) and Zhang et al. (2014) applied common average reference (CAR) before computing PLV. A discrete Laplacian spatial filter was applied by Hamner et al. (2011) to measure PLV and phase difference as control signals.

These methods of eliminating volume conduction are not perfect solutions. By eliminating zero-phase information, the imaginary part of coherence and phase-lag index are insensitive to true synchronization near zero phase. Even though volume conduction will produce zero-phase difference, not all zero-phase coupling is due to volume conduction (Gollo et al., 2014; Rajagovindan and Ding, 2008). Likewise, Thatcher (2012) and Nunez et al. (1997) suggest that spatial filtering may distort EEG signals by mixing phase differences between electrodes. It seems that spatial filtering with the Laplacian may underestimate coherence (Nunez et al., 1999). Brunner et al. (2006) also suggested to use ear-referenced EEG data when applying PLV as control feature after comparing with the result of applying spatial filters.

The goal of this study was twofold. One was to find the best PLV feature in SMR task based on EEG data for the application of real time BCI especially for a binary BCI task. Since the results show that the best PLV feature is coupling predominantly at zero-phase difference, we further explored whether this zero-phase PLV is due to volume conduction. The other goal of the present study was to investigate the effects of spatial filtering on PLV feature because it is widely applied as control feature in BCI studies. There are different opinions about whether spatial filtering should be applied as pre-processing method in computing PLV (Wei et al., 2007; Zhang et al., 2014; Hamner et al., 2011; Brunner et al., 2006). According to the results shown in this paper, there is significant zero-phase PLV feature based on ear-referenced data for task prediction involves the electrodes in the supplementary area and those in the primary motor area (M1). However, the large Laplacian largely eliminated this PLV feature by adding that information into amplitude feature. These results provide insights for BCI study.

2. Material and methods

2.1. Data recording

This study was based on a part of archival EEG data, the results of which have been previously reported (McFarland et al., 2000). Thirty-two of the original thirty-three subjects were involved in the present study using data from left hand and right hand movement tasks together with resting states. The data of the thirty-third subject was eliminated due to an insufficient number of trials. EEG data of 64 channels were sampled at 128 Hz referenced to the right ear and stored for offline analysis. Subjects were asked to try to avoid blinking and to actually move their left or right hand according to the location of a bar on the video screen. For example, when the bar appeared at the left edge of the screen, they repeatedly opened and closed their left hand. During the inter-trial interval when the screen was blank, subjects were simply relaxed (resting state). The experimental paradigm was detailed in (McFarland et al., 2000). There are three actual movement runs for each subject. Each run lasted approximately 2 min and contained left hand movement, right hand movement and rest tasks. For each subject, there were around 20 trials for left hand movement, 20 trials for

Table 1
Locations and largest r values (r_{BP}, r_{PLV}) in beta rhythm band for movement versus rest.

Location (BP)	r_{BP}	Location 1 (PLV)	Location 2 (PLV)	r_{PLV}
FCz	0.15	CP3	C4	−0.30

right hand movement and around 40 trials for resting states (the interval between left and right hand movement tasks). The duration of each trial (left hand movement, right hand movement, and rest) was around 4 s.

2.2. Feature extraction

In order to measure the degree of synchronization in EEG signals using PLV, a finite impulse response (FIR) filter (type I) and Hilbert transformation were applied. For example, for beta rhythm band PLV extraction, the EEG signals were first band-pass filtered by FIR beta rhythm bands ([18,25] Hz, FIR order = 24). Then, PLV was computed by choosing each of the 64 channels as the "seed channel" to which the other 63 channels were coupled with. PLV was computed according to

$$PLV = e^{j(\varphi_i - \varphi_j)}, \quad (1)$$

where $\langle \rangle$ stands for measuring the mean value of the computed window. φ_i, φ_j are the phase of EEG signals of channel i and j, computed by the Hilbert transformation.

We also measured the amplitude feature (square root of band power, BP) using the *bandpower* function in MatlabR2013 (MathWorks, Natick, MA, USA) based on the power spectral density estimation (PSD) of an autoregressive method (AR) (Marple, 1987) (AR order = 16, McFarland and Wolpaw, 2008).

Both BP and PLV features were extracted every 50 ms from the past 400 ms. Both features were the average of all the values of each 400 ms window for one trial. When studying the effects of spatial filtering on PLV, we computed BP and PLV feature using both ear referenced data (ear-referenced condition) and data pre-processed by a large Laplacian (large Laplacian condition).

2.3. Regression analysis

We measured the Pearson's correlation (Draper and Smith, 2014) between EEG features (BP, PLV or their combination) series $X = (x_i, 1 \leq i \leq N)$ and task indices (-1 for movement task, +1 for resting state) series $Y = (y_i, 1 \leq i \leq N)$ by:

$$r = \Sigma_{i=1}^N (S_i \cdot L_i) / \left(\sqrt{\Sigma_{i=1}^N S_i^2} \cdot \sqrt{\Sigma_{i=1}^N L_i^2} \right) \quad (2)$$

where $S_i = x_i - \left(\sum_1^N x_i \right) /N, L_i = y_i - \left(\sum_1^N y_i \right) /N$.

We first calculated r values for movement task (combining both left and right hand movement) versus rest for all 64 channels in beta rhythm bands, the goal of which was to find channels of interest in the study of BP and PLV (Table 1). There are 1239 trials for movement task, and 1236 trials for rest when combing data for all 32 subjects. The r_{BP} is the correlation between BP of each channel and SMR (beta rhythm) task indices (e.g. −1 for movement task, and +1 for resting state). The r_{PLV} is the correlation between PLV of each channel coupled and SMR task (-1 for movement, and +1 for resting state).

CP3, C4 and FCz channels were chosen as the channels of interest in this study according to Table 1 and the results as previously described (Chung et al., 2012; Wang et al., 2006; Yi et al., 2016). Therefore, BP feature of CP3, C4 and FCz and PLV feature of FCz coupling with CP3, FCz coupling with C4, and CP3 coupling with C4
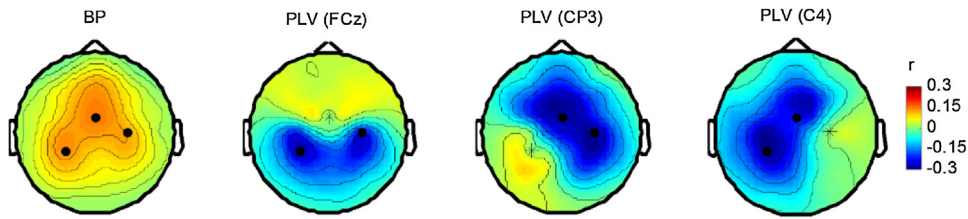
Fig. 1. Topographies of r_{BP}, where BP features of all channels were calculated with ear-referenced data and topographies of r_{PLV}, where PLV features were measured with ear-referenced data using either FCz, CP3, or C4 as the seed channels respectively for beta bands (18–25 Hz) comparing movement tasks with rest. Larger r_{BP}(red) corresponds to smaller BP (event-related desynchronization, ERD) during movement task comparing with that in resting state. Smaller r_{PLV} (blue) means PLV increasing during movement comparing with that in the resting states. FCz, CP3 and C4 are black dot-marked or star-marked if they are selected as the seed channel for computing PLV. (For interpretation of the references to colour in this figure legend, the reader is referred to the web version of this article.)
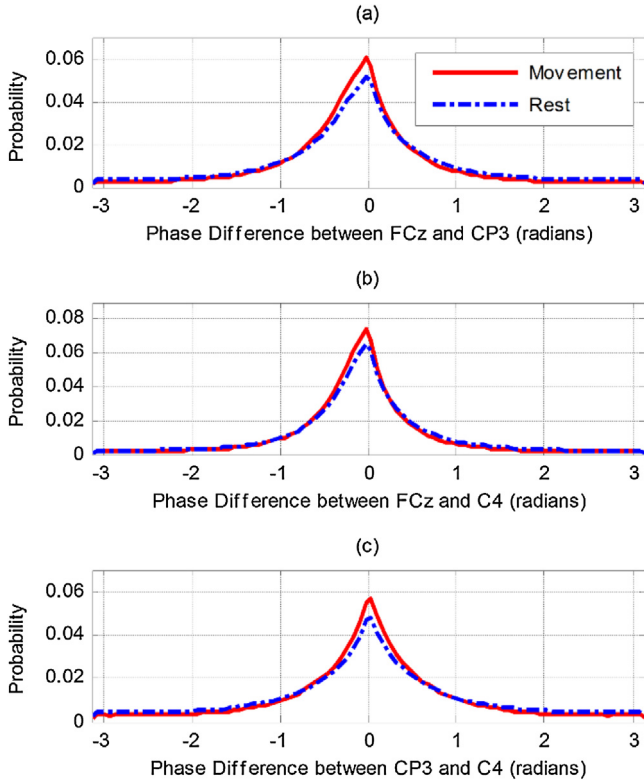

Fig. 2. Probability distributions of phase difference between FCz and CP3 (a), FCz and C4 (b), CP3 and C4 (c) for movement task and rest in beta rhythm band for all 32 subjects. There are 90 bins and the size of each equals 0.0698 rad. The maximum probability of (a)(b)(c) correspond to the phase difference at −0.0353, −0.0353, and 0.0353, respectively for both movement and rest.

were chosen to study the effects of large Laplacian. The r^2 values obtained from multiple regression with BP, PLV feature, and the combined feature of BP and PLV in large Laplacian condition were compared with that in ear-referenced condition. Furthermore, we computed unique and common covariance as described by Nimon et al. (2008) to determine the variance uniquely accounted for by BP and PLV.

We used multiple regression since it allows us to partition the variance between common and unique effects. The following is a brief introduction to the method for partitioning variance in multiple regression into common and unique components. If we regard the BP feature of FCz, CP3 and C4 channels as a single independent variables x_1, x_2, x_3, and PLV feature of FCz coupling with CP3, FCz coupling with C4, and CP3 coupling with C4 as the other independent variables x_4, x_5, x_6, then we have three multivariate models (multiple regression) based on BP ($X_{BP} = (x_1, x_2, x_3)$),

PLV ($X_{PLV} = (x_4, x_5, x_6)$), and both BP and PLV combined features ($X_{CF} = (x_1, x_2, x_3, x_4, x_5, x_6)$), respectively:

$$Y = b_1 * x_1 + b_2 * x_2 + b_3 * x_3 + a_1, \tag{3}$$

$$Y = b_4 * x_4 + b_5 * x_5 + b_6 * x_6 + a_2, \tag{4}$$

$$Y = b_7 * x_1 + b_8 * x_2 + b_9 * x_3 + b_{10} * x_4 + b_{11} * x_5 + b_{12} * x_6 + a_3, \tag{5}$$

The total variance accounted for X_{CF} ($r^2_{Y,X_{CF}}$) is given by Eq. (5). And the variance accounted for X_{BP} ($r^2_{Y,X_{BP}}$) and X_{PLV} ($r^2_{Y,X_{PLV}}$) is given by Eqs. (3) and (4), respectively.

The variance unique to BP features ($U_{X_{BP}}$) is given by (5)-(4):

$$U_{X_{BP}} = r^2_{Y,X_{CF}} - r^2_{Y,X_{PLV}}, \tag{6}$$

The variance unique to PLV features ($U_{X_{PLV}}$) is given by (5)-(3):

$$U_{X_{PLV}} = r^2_{Y,X_{CF}} - r^2_{Y,X_{BP}}, \tag{7}$$

The shared variance ($C_{X_{BP},X_{PLV}}$) between X_{BP} and X_{PLV} is given by

$$C_{X_{BP},X_{PLV}} = r^2_{Y,X_{CF}} - U_{X_{BP}} - U_{X_{PLV}}, \tag{8}$$

All the statistical tests based on the dependent variables (PLV or r^2) were done in SAS with repeated ANOVAs and Tukey's post hoc tests. The offline analysis of the EEG data was realized in Matlab2013.

3. Results

3.1. BP and PLV feature in beta rhythm band

We computed the r_{BP} (vector of 1*64) of all channels and r_{PLV} (a matrix of 64*64, by treating all 64 channels as seed channel, respectively) of all PLV couplings and chose the best channels corresponding to the largest absolute r_{BP} and r_{PLV} values. Table 1 gives the locations and the values of maximum r_{BP} and minimum r_{PLV} at the center of beta foci for movement versus rest. For movement task, beta desynchronization is maximum at FCz. The PLV coupling between CP3 and C4 shows the largest increasing among all PLV pairs. Fig. 1 shows average r_{BP} and r_{PLV} (PLV computed by regarding channel FCz, CP3 and C4 as the seed channel, respectively) for all subjects for movement versus rest. BP decreased over central sites with movement tasks in beta rhythm band. In contrast, PLV between FCz, CP3 and C4 increased with movement tasks compared with resting state. Thus, BP and PLV changed in opposite directions with movement tasks.

In summary, Fig. 1 shows that the effects of movement tasks for both BP and PLV mainly involve channels in anterior and M1 sites. However, these effects were in opposite directions for BP and PLV, consistent with the opposite sign of the r_{BP}, r_{PLV} shown in Table 1.
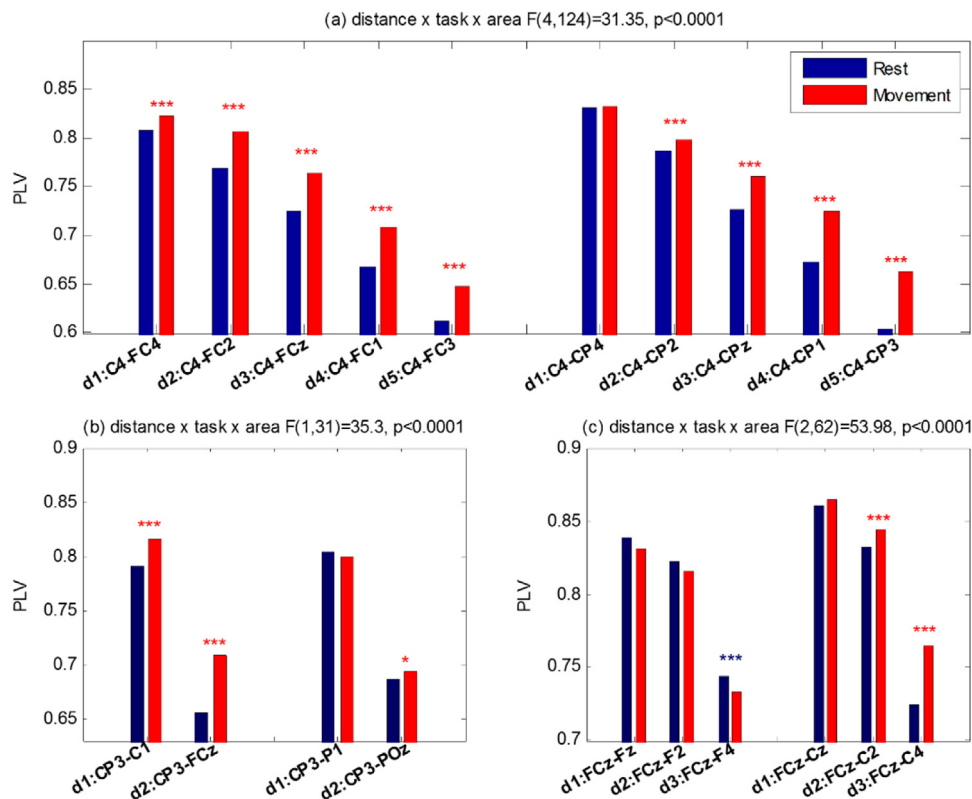
Fig. 3. (a) PLV of seed channel C4 coupling with anterior/posterior electrodes for five different distances (d1: C4-FC4/CP4; d2: C4-FC2/CP2; d3: C4-FCz/CPz; d4: C4-FC1/CP1; d5: C4-FC3/CP3); (b) PLV of seed channel CP3 coupling with anterior/posterior electrodes for two different distances (d1: CP3-C1/P1; d2: CP3-FCz/POz); (c) PLV of seed channel FCz coupling with anterior/posterior electrodes for three different distances (d1: FCz-F4/C4; d2: FCz-F2/C2; d3: FCz-Fz/Cz). Three-way repeated ANOVA resulted in a significant interaction between "task", "coupling area" and "distance" for (a)-(c). Tukey's post hoc test results show significant task-related effect, the significance level of which were shown by stars. * indicates $p < 0.05$, ** indicates $p < 0.001$ and *** indicates $p < 0.0001$. Bright red stars indicate that PLV of movement is significantly larger than that of rest. However, dark blue stars indicate that PLV of movement is significantly smaller than that of rest. (For interpretation of the references to colour in this figure legend, the reader is referred to the web version of this article.)

3.2. Zero-phase PLV and volume conduction

Given that coupling was increased between FCz, CP3 and C4 for movement compared with rest, we chose these three channels to investigate whether one channel was leading or lead by another. Fig. 2 shows that there was no leading source among those three channels, all of which were coupled at around zero-phase difference (-0.0353, −0.0353 and 0.0353 rad). Because volume conduction will also result in zero-phase difference, it was necessary to investigate whether these zero-phase effects represent meaningful long-distance coupling.

Fig. 3 shows the PLV feature of seed channel C4 (Fig. 3 (a)), CP3 (Fig. 3 (b)) and FCz (Fig. 3 (c)) coupling with electrodes in the anterior and posterior site (referring to the seed channel). Three-way repeated ANOVA involving "task" (two levels: movement, rest), "coupling area" (two levels: anterior, posterior) and "distance" (five levels in (a): d1, d2, d3, d4, d5; two levels in (b): d1, d2; three levels in (c): d1, d2, d3 (b)) show significant interaction ($F(4, 124) = 31.35$, $p < 0.0001$; $F(1, 31) = 35.3$, $p < 0.0001$; $F(2, 62) = 53.98$, p < 0.0001). Tukey's post hoc statistic tests show that as the distance to seed channel increases (Fig. 3(a)–(c)), the PLV feature decreases, which is consistent with volume conduction. Fig. 3(a) shows that there is general significant task-related effect for PLV of C4 coupling with anterior and posterior electrodes except for C4 coupling with CP4 in the posterior site, which is consistent with the r_{PLV} based topographies (with PLV computed by referring to C4) in Fig. 1. Fig. 3(b) shows that there is a significant task-related effect for CP3 coupling with electrodes C1 and FCz in anterior site (both at $p < 0.0001$), which does not occur

for the coupling with posterior electrodes (only a slight task-related effect for CP3 coupling with POz ($p < 0.05$)). Fig. 3(c) shows that PLV of FCz coupling with electrodes in posterior site (e.g., C2, C4) show significant task-related effect (PLV of movement is larger than that of rest, both at $p < 0.0001$) which does not occur for the coupling with anterior electrodes (e.g., Fz, F2, F4). This task-related effect occurs in anterior sites but not in posterior sites referring to CP3 in Fig. 3(b) and in posterior sites but not in anterior sites referring to FCz in Fig. 3(c). This asymmetry cannot be explained by volume conduction which would produce symmetrical effects.

These effects can be summarized by considering task independent effects (i.e., summed over task conditions) and task-dependent effects (i.e., the difference between task conditions). The overall PLV effects of distance on the sum and difference between movement task and rest are shown in Fig. 4 for both effects illustrated in Fig. 3. There are significant main effects of distance on sum of PLV value at $F(2, 62) = 22.53$, $p < 0.0001$; $F(2, 62) = 66.64$, $p < 0.0001$; $F(4, 124) = 168.42$, $p < 0.0001$, for Fig. 4 (a), (b) and (c), respectively. The sum of the PLV decreases when distance increases (Fig. 4 (a)-(c) black solid line). There are also significant main effects of distance on the difference of PLV at $F(2, 62) = 22.69$, $p < 0.0001$; $F(2, 62) = 46.34$, $p < 0.0001$; $F(4, 124) = 61.95$, $p < 0.0001$ for Fig. 4(a)–(c) respectively. However, the difference of PLV increases when the distance increases (Fig. 4(a)–(c) red dashed line). Fig. 4 shows that there is a task-independent reduction in PLV (sum) with distance as well as a task-dependent increase in PLV (difference) with distance from the seed electrode. While the task-independent effect of distance
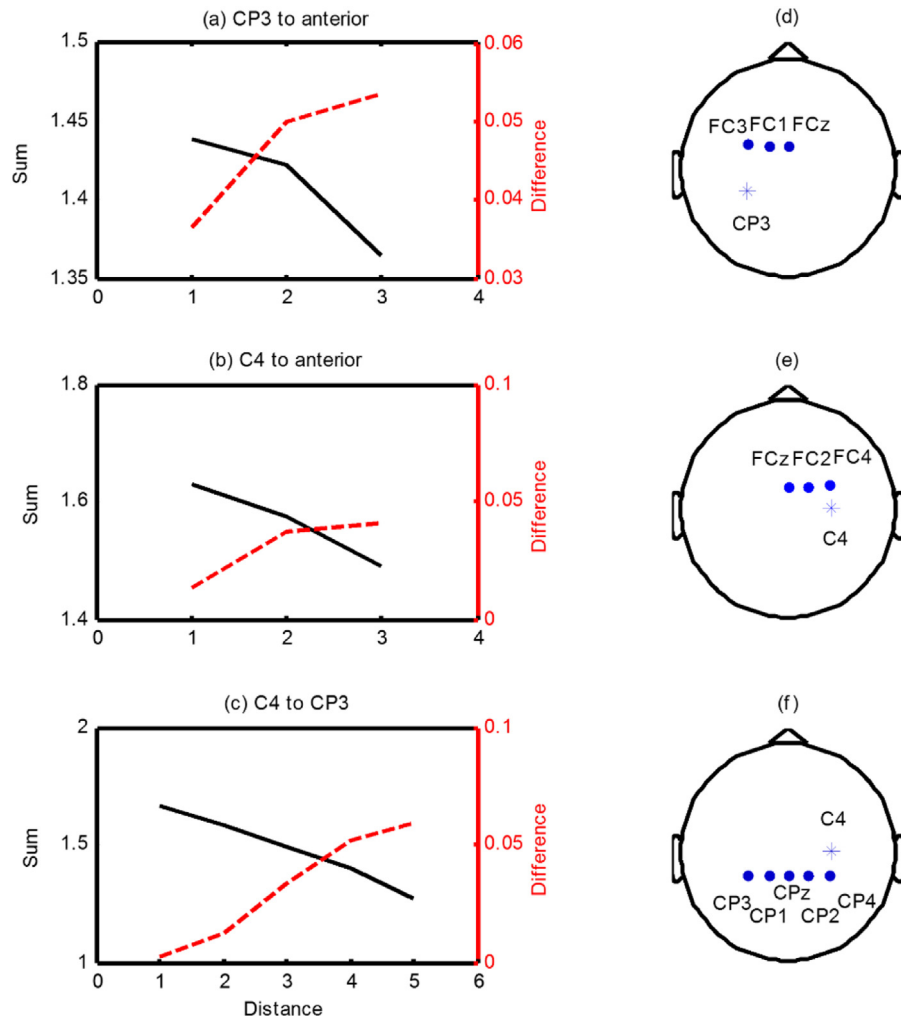
Fig. 4. Effects of distance on the sum and difference between PLV for movement task and rest for all 32 subjects for seed channel CP3/C4 coupling with anterior electrodes (d1: CP3 −FC3 or C4-FC4, d2: CP3-FC1 or C4-FC2, d3: CP3-FCz or C4-FCz) for (a), (b) respectively (corresponding involved channels shown in (e)(f), respectively) and C4 coupling with posterior electrodes (d1: C4-CP4, d2: C4- CP2, d3: C4-CPz, d4: C4-CP1, d5: C4-CP3) for (c) (corresponding involved channels shown in (g)). Panels (a)-(c) show that the summed PLV between movement and rest decreases when the distance increases (black solid line- task independent effects). However, the difference of PLV between actual movement tasks and rest increases when the distance increases (red dashed line- task dependent effects). (For interpretation of the references to colour in this figure legend, the reader is referred to the web version of this article.)

on PLV is consistent with volume conduction, the task-dependent effect is not.

In order to rule out the possibility that the zero-phase PLV feature is due to the contribution of lower-frequency (movement-related potentials) EEG data because of the spectral leakage, we also investigated the lower-frequency ([2,4] Hz, [5,7] Hz) and mu rhythm band ([9,13] Hz) PLV. Fig. 5 shows the topographies of r_{BP} and r_{PLV} with PLV computed by regarding FCz, CP3 and C4 as seed channel in lower frequencies for movement task versus resting state. Fig. 5 top and middle panels show that the target prediction abilities (r_{PLV} values) based on PLV (in [2,4] and [5,7] Hz) coupling with seed channel FCz, CP3 and C4 are largely decreased compared with that based on PLV computed in mu (Fig. 5 bottom panel) and beta rhythm band (Fig. 1). Meanwhile, the r_{BP} values in [2,4] and [5,7] Hz, especially at CP3, FCz and C4, are much smaller compared with that in beta rhythm band (Fig. 1). Fig. 5 bottom panel shows that for mu rhythm band, there is BP decrease in M1 and PLV increase for the coupling between M1 and anterior site, similar as that shown in Fig. 1 (beta rhythm band).

Fig. 6 shows the PLV feature of couplings between C4 and CP3, C4 and FCz, CP3 and FCz in four different frequency bands for both movement and rest tasks. A three-way repeated ANOVA involving

"task" (two levels: movement, rest), "coupling pair" (three levels: C4-CP3, C4-FCz, CP3-FCz) and "frequency band" (four levels: [2,4], [5,7], [9,13] and [18,25] Hz) show significant three-way interaction $F(6, 186) = 4.39$, $p < 0.0004$. Tukey's post hoc statistic tests show that only for mu and beta rhythm band, there is significant PLV increase for movement compared with rest (all at $p < 0.0001$ for all three coupling pairs). However, this phenomenon does not occur for PLV computed in [2,4] and [5,7] Hz. In summary, both Fig. 5 and Fig. 6 show that the movement-related lower frequency EEG data (e.g., [2,4] Hz, and [5,7] Hz) contribute little to the zero-phase PLV shown in sensorimotor rhythm band.

3.3. The effects of large laplacian on BP and PLV

Section 3.1 and 3.2 indicate that the increased PLV during actual movement is likely not due to volume conduction and that there is little contribution of low frequencies PLV for the task-related PLV. We next sought to determine whether PLV (e.g., in beta rhythm band) provides useful information for predicting task-related effects in addition to the BP feature. Multiple regressions were computed individually for each subject with task (movement versus rest) as the dependent variable and BP features (FCz, CP3, and
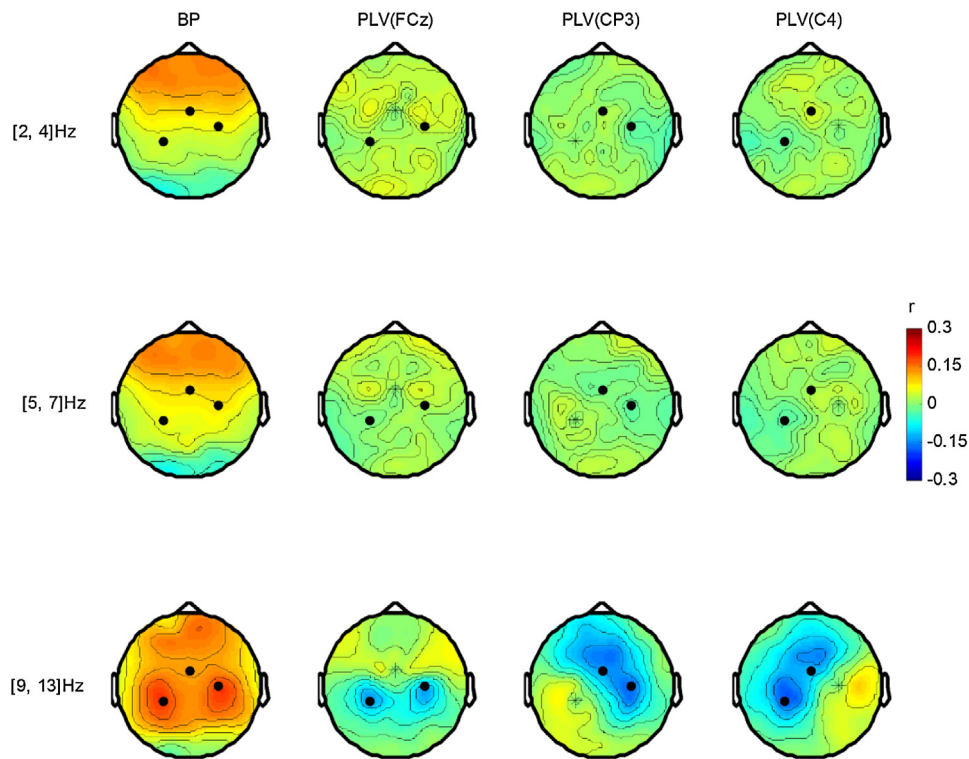
Fig. 5. The r_{PLV} based topographies for movement versus rest in lower frequency bands (e.g., [2,4]Hz, [5,7] Hz) and mu rhythm band ([9,13]Hz). PLV were computed with star-marked coupled channel FCz, CP3 and C4, respectively. FCz, CP3 and C4 are dot-marked if they are not selected as the seed channel. The seed channel for computing PLV is star-marked in the topographies.
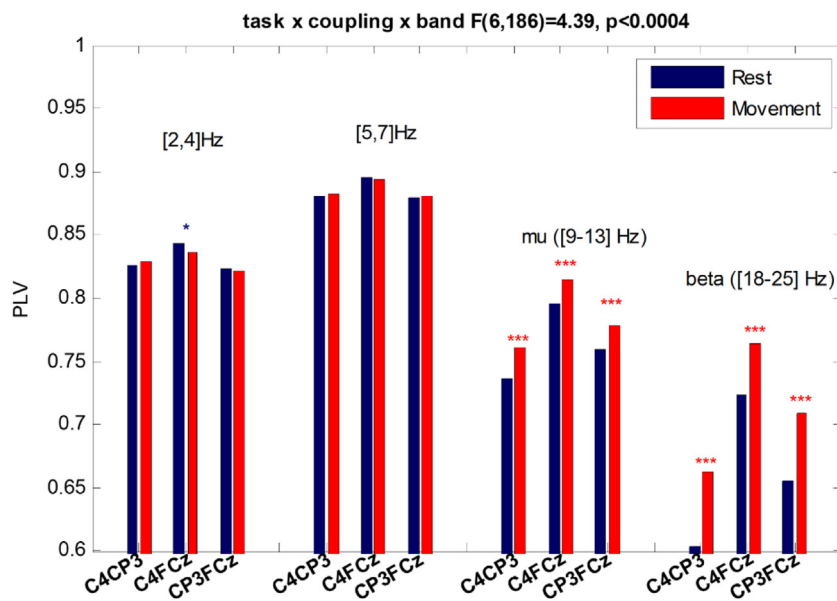

Fig. 6. PLV of three coupling pairs (C4-CP3, C4-FCz, CP3-FCz) in four different frequency bands ([2,4], [5,7], [9,13] and [18,25] Hz). Bright red stars indicate that PLV of movement is significantly larger than that of rest. However, dark blue star indicates that PLV of movement is significantly smaller than that of rest. (For interpretation of the references to colour in this figure legend, the reader is referred to the web version of this article.)

C4), PLV features (FCz coupling with CP3 and C4, and CP3 coupling with C4) or combined features of BP and PLV as independent variables. Features were computed for both ear-referenced and large Laplacian conditions in order to assess the effects of large Laplacian on phase feature.

Because BP and PLV might be correlated with each other, we did a commonality analysis. Fig. 7 shows the r^2 value based on unique BP, unique PLV and their common covariance with task condition

for movement versus rest. The maximum r^2 value based on the common part of BP and PLV was less than 0.09, which indicates that the common covariance of BP and PLV with task condition was small and that the association of the two with movement are independent sources of variance. A two-way repeated ANOVA with the r^2 values for the regression analyses as the dependent variable and "condition" (two levels: large Laplacian condition, ear-referenced condition), "Feature type" (four levels: unique BP,
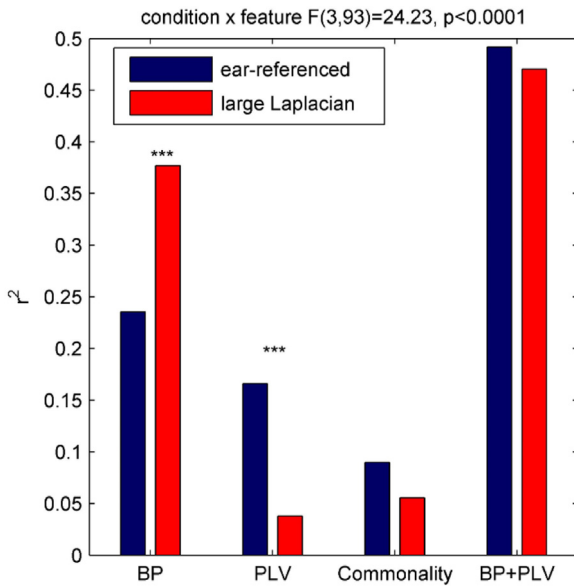
Fig. 7. The r^2 value for prediction of task condition based on unique BP, unique PLV, the common part of BP and PLV (Commonality), and combined feature (BP + PLV) of BP and PLV for movement versus rest in both ear-referenced and large Laplacian conditions.

Fig. 8. BP ("local PLV") of FCz (the vertices of the triangle), CP3 (bottom left) and C4 (bottom right) areas decreasing with motor execution (red arrow) and "long-distant PLV" increasing with motor execution (blue arrow) between CP3/C4 and FCz, and between CP3 and C4. (For interpretation of the references to colour in this figure legend, the reader is referred to the web version of this article.)

unique PLV, common part of BP and PLV (Commonality), combined feature of BP and PLV(BP + PLV)) as independent variables produced significant interaction ($F(3, 93) = 24.23$, $p < 0.0001$). Tukey's post hoc analysis showed that the r^2_{BP} value in large Laplacian condition is larger than that in ear-referenced condition ($p < 0.0001$). In the contrast, r^2_{PLV} in large Laplacian condition is smaller than that in ear-referenced condition ($p < 0.0001$). Interestingly, there is no significant difference between r^2_{CF} in ear-referenced and large Laplacian conditions (p = 0.98), but r^2_{CF} is significantly larger than r^2_{BP} and r^2_{PLV}, respectively, for both large Laplacian ($r^2_{CF} > r^2_{BP}$ at p < 0.0021, and $r^2_{CF} > r^2_{PLV}$ at p < 0.0001) and ear-referenced conditions ($r^2_{CF} > r^2_{BP}$ and $r^2_{CF} > r^2_{PLV}$ both at p < 0.0001). The r^2 value based on the commonality part of BP and PLV have no significant difference in ear-referenced and large Laplacian condition.

Thus, the PLV feature provided an independent source of information for task prediction. Fig. 7 demonstrates that unique PLV for task prediction was significantly eliminated and that the unique BP feature was enhanced when a large Laplacian was applied. In other words, the large Laplacian combines both amplitude and phase effects, enhancing BP and eliminating information in PLV.

4. Discussion

The findings of this study based on EEG data for 32 untrained subjects involving left and right hand movement tasks show that zero-phase PLV between FCz and CP3, C4 and between CP3 and C4 is not entirely due to volume conduction. This conclusion is supported by the fact that BP and PLV are modulated by task state in opposite directions and by the fact that the spatial gradients of task-related PLV effects increase with distance asymmetrically. If these effects were simply due to volume conduction, the increase in signal-to-noise ratio with an increase in BP would tend to produce an increase in PLV (Nikouline et al., 2001; Daffertshofer et al., 2011; Bayraktaroglu et al., 2013). Thus, the task-related component of PLV appears to represent real long-distance coupling. The other important finding of this study is that large Laplacian eliminates useful task-related information in PLV, presumably because it combines both amplitude and phase effects. This latter finding has potential implications for other spatial filtering operations as well.
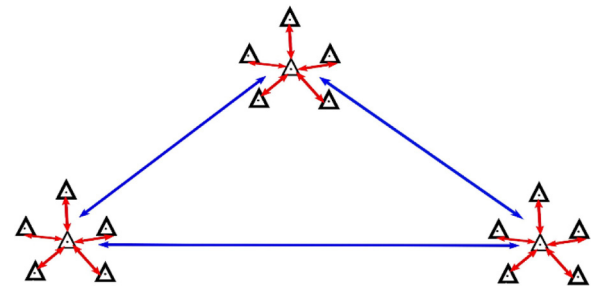
Although volume conduction will produce coupling at zero-phase difference, simulations suggest that zero-phase coupling can also be produced by common input from a third source or bi-directional communication between sources (Gollo et al., 2014; Rajagovindan and Ding, 2008). In order to eliminate effects of volume conduction, Witham et al. (2007) examined coherence between M1 field potentials and unit activity in somatosensory cortex of monkeys and observed many units synchronized around zero lag. Thus there are both theoretical rationales and empirical evidence suggesting that near zero phase lag coupling could represent real long-range coupling.

Activity recorder at a single scalp electrode represents synchronization between a local population of neurons of sufficient size to be detected at the scalp (Lopes da Silva, 2013). Thus, the BP measure can be regarded as a local coupling. The zero-phase coupling between FCz, CP3 and C4 that is a task-dependent modulation appears to be real long distance coupling. Fig. 8 provides a rational explanation of the opposition modulation of BP and PLV in the ear-referenced condition by task state and the different gradients of task-dependent and task-independent effects on PLV. Fig. 8 shows greater local synchronization in the rest condition that shifts to relatively greater long-range synchronization during movement.

Andrew and Pfurtscheller (1996) found that the phase coupling between C3 and C4 increase during a movement task. They suggested that this effect was due to volume conduction since it could be eliminated by applying a Laplacian filter. However, the present results argue against this interpretation since the task-related effect on PLV increases with increasing distance. This is opposite to the task independent effect and what would be predicted by volume conduction. Other studies investigating the functional connectivity for movement and imagery tasks with EEG data use spatial filters. For example, Bauer et al. (2015) investigated coupling during movement and imagery tasks by using EEG data preprocessed by independent component analysis, spline Laplacian and then principal component analysis. Each of these steps could potentially distort phase features. Therefore, applying spatial filters in EEG study involving phase information may obscure real zero-phase effects. Phase and amplitude effects could be combined by many different spatial filtering transforms, such as principal components, independent components, and common spatial patterns. Source localization is a non-linear transformation that could be influenced by phase effects.

Even though zero-phase coupling between FCz and CP3, FCz and C4, and CP3 and C4 seems to show significant task-related effects which cannot be explained by volume conduction, there are limitations to the current study. For example, suppose all three sources right below FCz, CP3 and C4 (amplitude decrease during movement tasks) as we suggested are asynchronous. Also suppose that there might be an additional source X (amplitude increase) in the brain,

that contributes also to FCz, CP3 and C4 electrodes. This might also lead to additional (non-redundant) information in PLV (the coupling between FCz, CP3 and C4 electrodes) about movement even though the effect is purely due to volume conduction. In this situation, the zero-phase PLV is likely due to volume conduction. However, this case is based on the assumption that three asynchronous individual sources contribute exclusively to FCz, CP3 and C4, respectively, which is contrary to the expectation of volume effects. Therefore, there are not perfect methods to totally eliminate the possibility of volume conduction effects due to the limitation of the scalp EEG recording method (Cohen, 2015b). Fig. 8 is an example only to illustrate the effects of what we have observed especially the opposite modulation of BP and PLV and the coupling predominantly at zero phase difference involving those three electrodes.

In this paper, we regarded the near-zero phase lag PLV as true reciprocal phase synchronization, which might be a simplest possibility. There are other more complicated source localization methods instead of using PLV feature to localize the source of EEG signals, such as brain electric source analysis (BESA) (Baillet, 1998) and low resolution electromagnetic tomography algorithm (LORETA)(Pascual-Marqui et al., 1994). However, those inverse techniques generally do not take phase into account and assume no synchrony between sources (Grech et al., 2008). What we observed in this paper is about reciprocal coupling at zero-phase, indicating that inverse techniques (e.g., LORETA) and directed methods such as directed transfer function and Granger Causality (Kamiński et al., 2001) targeting at directed coupling are not appropriate for this case.

5. Conclusion

This study found that zero-phase PLV is not totally due to volume conduction since it varies in a direction opposite to that of the BP feature in response to left and right hand movement tasks. In addition, this task-dependent effect on PLV increases with distance toward the contralateral electrode overlying the hand motor area. The task-dependent PLV effect is eliminated when the EEG data is pre-processed by a large Laplacian. At the same time, the large Laplacian combines amplitude and phase information.

Acknowledgements

References

Andrew, C., Pfurtscheller, G., 1996. Dependence of coherence measurements on EEG derivation type. Med. Biol. Eng. Comput. 34, 232–238.

Baillet, S., 1998. Toward Functional Imaging of Cortical Electrophysiology Markovian Models for the Source Estimation of Magneto/electroencephalography and Experimental Assessments. ResearchGate.

Bauer, R., Fels, M., Vukelić, M., Ziemann, U., Gharabaghi, A., 2015. Bridging the gap between motor imagery and motor execution with a brain-robot interface. Neuroimage 108, 319–327, http://dx.doi.org/10.1016/j.neuroimage.2014.12.026.

Bayraktaroglu, Z., von Carlowitz-Ghori, K., Curio, G., Nikulin, V.V., 2013. It is not all about phase: Amplitude dynamics in corticomuscular interactions. NeuroImage 64, 496–504, http://dx.doi.org/10.1016/j.neuroimage.2012.08.069.

Brunner, C., Scherer, R., Graimann, B., Supp, G., Pfurtscheller, G., 2006. Online control of a brain-Computer interface using phase synchronization. IEEE Trans. Biomed. Eng. 53, 2501–2506, http://dx.doi.org/10.1109/TBME.2006.881775.

Bullmore, E., Sporns, O., 2009. Complex brain networks: graph theoretical analysis of structural and functional systems. Nat. Rev. Neurosci. 10, 186–198, http://dx.doi.org/10.1038/nrn2575.

Carter, G., Knapp, C., Nuttall, A., 1973. Estimation of the magnitude-squared coherence function via overlapped fast Fourier transform processing. IEEE Trans. Audio Electroacoust. 21, 337–344, http://dx.doi.org/10.1109/TAU.1973.1162496.

Chung, Y.G., Kang, J.-H., Kim, S.-P., 2012. Correlation of fronto-central phase coupling with sensorimotor rhythm modulation. Neural Netw. 36, 46–50, http://dx.doi.org/10.1016/j.neunet.2012.08.006.

Cohen, M.X., 2015a. Comparison of different spatial transformations applied to EEG data: a case study of error processing. Int. J. Psychophysiol. 97, 245–257, http://dx.doi.org/10.1016/j.ijpsycho.2014.09.013, On the benefits of using surface Laplacian (current source density) methodology in electrophysiology.

Cohen, M.X., 2015b. Effects of time lag and frequency matching on phase-based connectivity. J. Neurosci. Methods 250, 137–146, http://dx.doi.org/10.1016/j.jneumeth.2014.09.005, Cutting-edge EEG Methods.

Daffertshofer, A., Wijk, V.M.B.C., 2011. On the Influence of Amplitude on the Connectivity between Phases. Front. Neuroinf. 5, http://dx.doi.org/10.3389/fninf.2011.00006.

Draper, N.R., Smith, H., 2014. Applied Regression Analysis. John Wiley & Sons.

Gollo, L.L., Mirasso, C., Sporns, O., Breakspear, M., 2014. Mechanisms of zero-lag synchronization in cortical motifs. PLoS Comput. Biol. 10, e1003548, http://dx.doi.org/10.1371/journal.pcbi.1003548.

Grech, R., Cassar, T., Muscat, J., Camilleri, K.P., Fabri, S.G., Zervakis, M., Xanthopoulos, P., Sakkalis, V., Vanrumste, B., 2008. Review on solving the inverse problem in EEG source analysis. J. Neuro Eng. Rehabil. 5, 25, http://dx.doi.org/10.1186/1743-0003-5-25.

Hamner, B., Leeb, R., Tavella, M., del, R., Millán, J., 2011. Phase-based features for motor imagery brain-computer interfaces. Conf. Proc. Annu. Int. Conf. IEEE Eng. Med. Biol. Soc. IEEE Eng. Med. Biol. Soc. Annu. Conf. 2011, 2578–2581, http://dx.doi.org/10.1109/IEMBS.2011.6090712.

Kamiński, M., Ding, M., Truccolo, W.A., Bressler, S.L., 2001. Evaluating causal relations in neural systems: granger causality, directed transfer function and statistical assessment of significance. Biol. Cybern. 85, 145–157, http://dx.doi.org/10.1007/s004220000235.

Lachaux, J.P., Rodriguez, E., Martinerie, J., Varela, F.J., 1999. Measuring phase synchrony in brain signals. Hum. Brain Mapp. 8, 194–208.

Lopes da Silva, F., 2013. EEG and MEG: relevance to neuroscience. Neuron 80, 1112–1128, http://dx.doi.org/10.1016/j.neuron.2013.10.017.

Marple Jr., S.L., 1987. Digital Spectral Analysis with Applications. American Scientist.

McFarland, D.J., Wolpaw, J.R., 2008. Sensorimotor rhythm-based brain?computer interface (BCI): model order selection for autoregressive spectral analysis. J. Neural Eng. 5, 155, http://dx.doi.org/10.1088/1741-2560/5/2/006.

McFarland, D.J., Miner, L.A., Vaughan, T.M., Wolpaw, J.R., 2000. Mu and beta rhythm topographies during motor imagery and actual movements. Brain Topogr. 12, 177–186, http://dx.doi.org/10.1023/A:1023437823106.

McFarland, D.J., Sarnacki, W.A., Wolpaw, J.R., 2010. Electroencephalographic (EEG) control of three-dimensional movement. J. Neural Eng. 7, 36007, http://dx.doi.org/10.1088/1741-2560/7/3/036007.

Nikouline, V.V., Linkenkaer-Hansen, K., Huttunen, J., Ilmoniemi, J.R., 2001. Interhemispheric phase synchrony and amplitude correlation of spontaneous beta oscillations in human subjects: a magnetoencephalographic study. Neuroreport 12 (11), 2487–2491, http://dx.doi.org/10.1097/00001756-200108080-00040.

Nimon, K., Lewis, M., Kane, R., Haynes, R.M., 2008. An R package to compute commonality coefficients in the multiple regression case: an introduction to the package and a practical example. Behav. Res. Methods 40, 457–466, http://dx.doi.org/10.3758/BRM.40.2.457.

Nolte, G., Bai, O., Wheaton, L., Mari, Z., Vorbach, S., Hallett, M., 2004. Identifying true brain interaction from EEG data using the imaginary part of coherency. Clin. Neurophysiol. 115, 2292–2307, http://dx.doi.org/10.1016/j.clinph.2004.04.029.

Nunez, P.L., Srinivasan, R., Westdorp, A.F., Wijesinghe, R.S., Tucker, D.M., Silberstein, R.B., Cadusch, P.J., 1997. EEG coherence: i: statistics, reference electrode, volume conduction, Laplacians, cortical imaging, and interpretation at multiple scales. Electroencephalogr. Clin. Neurophysiol. 103, 499–515, http://dx.doi.org/10.1016/S0013-4694(97)00066-7.

Nunez, P.L., Silberstein, R.B., Shi, Z., Carpenter, M.R., Srinivasan, R., Tucker, D.M., Doran, S.M., Cadusch, P.J., Wijesinghe, R.S., 1999. EEG coherency II: experimental comparisons of multiple measures. Clin. Neurophysiol. 110, 469–486, http://dx.doi.org/10.1016/S1388-2457(98)00043-1.

Nunez, P.L., Wingeier, B.M., Silberstein, R.B., 2001. Spatial-temporal structures of human alpha rhythms: theory, microcurrent sources, multiscale measurements, and global binding of local networks. Hum. Brain Mapp. 13, 125–164, http://dx.doi.org/10.1002/hbm.1030.

Nunez, P.L., Srinivasan, R., Fields, R.D., 2015. EEG functional connectivity, axon delays and white matter disease. Clin. Neurophysiol. 126, 110–120, http://dx.doi.org/10.1016/j.clinph.2014.04.003.

Pascual-Marqui, R.D., Michel, C.M., Lehmann, D., 1994. Low resolution electromagnetic tomography: a new method for localizing electrical activity in the brain. Int. J. Psychophysiol. 18, 49–65, http://dx.doi.org/10.1016/0167-8760(84)90014-X.

Pfurtscheller, G., Lopes da Silva, F.H., 1999. Event-related EEG/MEG synchronization and desynchronization: basic principles. Clin. Neurophysiol. 110, 1842–1857, http://dx.doi.org/10.1016/S1388-2457(99)00141-8.

Rajagovindan, R., Ding, M., 2008. Decomposing neural synchrony: toward an explanation for near-zero phase-lag in cortical oscillatory networks. PLoS One 3, e3649, http://dx.doi.org/10.1371/journal.pone.0003649.

Stam, C.J., van Straaten, E.C.W., 2012. The organization of physiological brain networks. Clin. Neurophysiol. 123, 1067–1087, http://dx.doi.org/10.1016/j.clinph.2012.01.011.

Stam, C.J., Nolte, G., Daffertshofer, A., 2007. Phase lag index: assessment of functional connectivity from multi channel EEG and MEG with diminished bias from common sources. Hum. Brain Mapp. 28, 1178–1193, http://dx.doi.org/10.1002/hbm.20346.

Tenke, C.E., Kayser, J., 2015. Surface Laplacians (SL) and phase properties of EEG rhythms: simulated generators in a volume-conduction model. Int. J. Psychophysiol. 97, 285–298, http://dx.doi.org/10.1016/j.ijpsycho.2015.05.008, On the benefits of using surface Laplacian (current source density) methodology in electrophysiology.

Thatcher, R.W., 2012. Coherence, phase differences, phase shift, and phase lock in EEG/ERP analyses. Dev. Neuropsychol. 37, 476–496, http://dx.doi.org/10.1080/87565641.2011.619241.

Wang, Y., Hong, B., Gao, X., Gao, S., 2006. Phase synchrony measurement in motor cortex for classifying single-trial EEG during motor imagery. In: 28th Annual International Conference of the IEEE Engineering in Medicine and Biology Society, 2006. EMBS #xps1#06. Presented at the 28th Annual International Conference of the IEEE Engineering in Medicine and Biology Society, 2006. EMBS '06, pp. 75–78, http://dx.doi.org/10.1109/IEMBS.2006.259673.

Wei, Q., Wang, Y., Gao, X., Gao, S., 2007. Amplitude and phase coupling measures for feature extraction in an EEG-based brain-computer interface. J. Neural Eng. 4, 120, http://dx.doi.org/10.1088/1741-2560/4/2/012.

Witham, C.L., Wang, M., Baker, S.N., 2007. Cells in somatosensory areas show synchrony with beta oscillations in monkey motor cortex. Eur. J. Neurosci. 26, 2677–2686, http://dx.doi.org/10.1111/j.1460-9568.2007.05890.x.

Wolpaw, J.R., McFarland, D.J., 2004. Control of a two-dimensional movement signal by a noninvasive brain-computer interface in humans. Proc. Natl. Acad. Sci. U. S. A. 101, 17849–17854, http://dx.doi.org/10.1073/pnas.0403504101.

Wolpaw, J.R., McFarland, D.J., Neat, G.W., Forneris, C.A., 1991. An EEG-based brain-computer interface for cursor control. Electroencephalogr. Clin. Neurophysiol. 78, 252–259, http://dx.doi.org/10.1016/0013-4694(91)90040-B.

Yi, W., Qiu, S., Wang, K., Qi, H., He, F., Zhou, P., Zhang, L., Ming, D., 2016. EEG oscillatory patterns and classification of sequential compound limb motor imagery. J. NeuroEngineering Rehabil. 13, http://dx.doi.org/10.1186/s12984-016-0119-8.

Zhang, J., Wang, N., Kuang, H., Wang, R., 2014. An improved method to calculate phase locking value based on Hilbert-Huang transform and its application. Neural Comput. Appl. 24, 125–132, http://dx.doi.org/10.1007/s00521-013-1510-z.